J. Electrochem. Sci. Eng. **00(0)** (2024) 000-000; http://dx.doi.org/10.5599/jese.2467

Open Access : : ISSN 1847-9286
www.jESE-online.org

Original scientific paper

Electrochemical impedance spectroscopy measurements on time-variant systems: the case of the Volmer-Heyrovský corrosion reaction. Part I: theoretical description

Nicolas Murer✉, Jean-Paul Diard and Bogdan Petrescu

BioLogic, 4 Rue de Vaucanson, 38170 Seyssinet-Pariset, France

Corresponding authors: ✉nicolas.murer@biologic.net; Tel.: +33-476-986-831

Received: August 13, 2024; Accepted: September 10, 2024; Published: September 20, 2024

Abstract

One of the theoretical requirements of electrochemical impedance spectroscopy measurements is that the studied system should not vary with time. Unfortunately, this is rarely the case of physical systems. In the literature, quite a few methods exist to check and correct a posteriori the effect of time-variance, allowing the use of conventional equivalent circuit models to fit and interpret the data. We suggest a different approach where, for a given electrochemical mechanism and specific experimental conditions, assuming stationarity during each measurement, a time- and frequency-dependent expression of the Faradaic impedance is derived from the kinetic equations. The case of a potential relaxation at zero current following an anodic steady-state polarization is considered for a system where a Volmer-Heyrovský corrosion mechanism is supposed to take place.

Keywords

EIS; adsorption; non-stationarity; Faradaic; relaxation; potential decay

Introduction

Electrochemical impedance spectroscopy (EIS) consists of studying the frequency response of an electrochemical system submitted to an electrical modulation, leading to the determination of its transfer function, the involved electrochemical reaction mechanisms and the values of the associated parameters.

Classically, the Faradaic impedance of a given electrochemical reaction is obtained by linearizing the expression of the Faradaic current using a Taylor series limited to the first order in the neighbourhood of a stationary operating point [1].

This means that the electrical perturbation applied to the system where the given electrochemical reaction takes place should not entail a nonlinear response.

This also means that the system should be stationary. As already noted elsewhere [2,3], it is considered by the authors that stationarity includes two sub-notions, namely steady-state and time-

invariance. Steady-state is the state of a system whose response has reached a permanent regime and time-invariance is the state of a system whose parameters do not change with time.

A complete description, or at least a study, of an electrochemical reaction mechanism requires impedance measurements performed at various stationary points along the stationary *I vs. E* curve. This is generally performed by collecting impedance data after the system has settled at a constant potential.

However, in some systems, the waiting time to reach the stationary state can be considered too long, for example, in the case of an insertion battery or a corroding sample. Besides, strictly speaking, no stationary state can really be defined for those systems as the voltage measured across a battery and the mixed potential measured on a corroding electrode are not equilibrium thermodynamic potentials, so the stationary approach is not deemed relevant.

A third example is given by Harrington *et al.* [4] in the case of methanol oxidation, whose irreversible adsorption reaction leads to a full-coverage state, whichever the applied potential.

In such cases, there is no other way than to perform impedance measurements in non-stationary conditions, which goes against the requirement mentioned above unless some precautions, assumptions and corrections are taken and applied.

Stoynov *et al.* [5] were the first to knowingly perform EIS measurements on a time-variant system, namely a lead-acid battery under discharge. By choosing a low enough current and keeping the measurement time short, it was assumed that the system would not change very much during the measurement and was considered to be in a quasi-stationary state (QSS).

This is also the approach chosen by researchers combining voltammetry and EIS in techniques such as potentiodynamic DEIS [6], ac voltammetry [4,7] and dynamic EIS [8-11].

The QSS or “frozen-state” assumption allows to use, at each frequency, conventional equivalent circuit models (ECM) and Faradaic impedance expressions to interpret the data, but the values of the parameters could differ from one frequency to another.

Stoynov was, to our knowledge, the first to simulate how non-stationarity can deform impedance Nyquist diagrams and lead to wrong interpretations [12]. Stoynov *et al.* introduced an elegant correction method named 4D impedance based on the cubic spline interpolation of successive measurements, allowing for a reconstruction of instantaneous impedance spectra, which can then be interpreted using conventional ECM with time-independent parameters [13,14]. More recently, the same authors introduced the rotating Fourier transform [15,16] to directly analyze non-stationary impedance measurements without the need for correction.

Belgian researchers developed a methodology using odd multisine signals (Odd random phase multisine EIS (ORP-EIS)) to quantify the non-linearity and non-stationarity of nonlinear time-varying systems [17,18]. Non-linearities appear as additional signals at non-excited frequencies and time-variance appears as “jumps” or “skirts” at excited frequencies.

The different types of Fourier spectra of the response to sinusoidal excitation are presented in the white paper “Systems and EIS quality indicators” [19]. Non-linearity and non-stationarity indicators are also presented.

This non-exhaustive review gives an idea of the various approaches used to tackle the problem of non-stationarity. Other approaches and more details can be found in two recent review articles by Hallemans *et al.* [20] and Szekeres *et al.* [21].

These approaches all rely on a mathematical treatment of the EIS measurement, using the point of view of the physicist or the signal analyst. The point of view of the electrochemist was adopted

here, starting from the electrochemical reaction and the kinetic equations to the calculation of a time and frequency-dependent Faradaic impedance expression.

The first attempt originated from a paper by the team of Srinivasan Ramanathan, who illustrated the effect of time-variance by performing impedance measurements on a rotating disk electrode (RDE) immersed in an electrolyte containing equimolar concentrations of the classical ferri- and ferrocyanide ions and being diluted [22]. In our recent paper [2], the time and frequency-dependent Faradaic impedance expression was calculated for such a redox reaction where the concentration changes with time and showed that it was possible to use this expression to fit experimental impedance data obtained on the time-variant system directly.

The topic of linear systems with variable parameters was also studied by Berthier [23], who recalled that the main issue is that, unless the system is simple, there is no mathematical method available to solve the differential Equation (1) describing the system, which is:

$$a_n(t)y^n(t) + a_{n-1}(t)y^{n-1}(t) + \cdots + a_1(t)y'(t) + a_0(t)y(t) = b_m(t)u^m(t) + \cdots b_0(t)u(t) \quad (1)$$

where $y^n(t)$ represents the n^{th} time derivative of the function $y(t)$, $u^m(t)$ represents the m^{th} time derivative of the function $u(t)$, $y(t)$ is the time response of the considered system and $u(t)$ the time input with $a(t)$ and $b(t)$ their respective time-dependent coefficients.

Baddi [24] tried to explain the passivation mechanism of iron in an acidic medium as well as the time evolution of the potential during depassivation, also named the Flade experiment. In this experiment, a constant stationary passivation current or potential is applied to the system, the current is then shut and the potential returns to its equilibrium value. This potential time evolution is calculated by using the various kinetic equations derived from the chosen depassivation mechanism. The non-stationary impedance expression is written using the stationary, voltage-dependent impedance expression and replacing the stationary voltage with the time-dependent voltage.

Harrington [25] calculated open-circuit potential decay transients following the interruption of a polarizing current for a three-step hydrogen evolution reaction (HER) and related to the evolution of the surface coverage rate of the adsorbed species.

In this paper, we chose to follow a similar approach using as a case study the Volmer-Heyrovský corrosion reaction [26-28, and references therein]. This first part shows the theoretical derivation, while the second part, to be published, will present experimental data.

Mechanism and kinetic equations

The notation and the equations of the Handbook of Electrochemical Impedance Spectroscopy Corrosion Reactions Library [29] were used.

Each reaction is considered non-inversible or irreversible, meaning the forward reaction rate is much larger than the backward reaction rate.

The two-step hydrogen reduction reaction is considered, Equations (2) and (3):

$$H^+ + s + e^- \xrightarrow{K_{r1}} H,s \quad (2)$$

$$H^+ + H,s + e^- \xrightarrow{K_{r2}} H_2 + s \quad (3)$$

with s an adsorption site, K_{r1} in s^{-1} and K_{r2} in s^{-1} the reaction rate constants. H,s denotes an adsorbed H atom (or H adatom).

The oxidation reaction is the corrosion of the metal atom at the surface of the electrode M.s, which produces, in our case, for the sake of simplicity, a divalent species M^{2+} (Equation (4)):

$$M,s \xrightarrow{K_{o3}} M^{2+} + s + 2e^- \quad (4)$$

with K_{o3} / s^{-1} the reaction rate constant.

M,s and s are considered to be equivalent, which means the oxidation reaction does not lead to a variation in surface concentration of the adsorption sites.

The Langmuir isotherm is used, which means that there are no interactions between the adsorbed species, which are assumed to form an ideal condensed phase.

There is no mass transport limitation, which means that interfacial concentrations $H^+(0,t)$ are equal to bulk concentrations H^{+*}, or that interfacial concentration variations are negligible, Equation (5):

$$H^+(0,t) \approx H^{+*} \tag{5}$$

This allows us to write Equations (6) to (8):

$$K_{r1}(t) = k_{r1}\exp\left(-\alpha_{r1} f_N E(t)\right), k_{r1} = k'_{r1} H^{+*} \tag{6}$$

$$K_{r2}(t) = k_{r2}\exp\left(-\alpha_{r2} f_N E(t)\right), k_{r1} = k'_{r1} H^{+*} \tag{7}$$

$$K_{o3}(t) = k_{o3}\exp\left(2\alpha_{o3} f_N E(t)\right) \tag{8}$$

with $f_N = F/(RT)$, F = 96485 C mol^{-1} the Faraday constant, R = 8.32 J mol^{-1} K^{-1} the perfect gas constant, T in K the absolute temperature, k_{r1} in s^{-1} and k_{r2} in s^{-1} the transfer kinetic parameters of the reduction reactions, k_{o3} in s^{-1} the transfer kinetic parameter of the oxidation reaction, a_{r1}, a_{r2} and a_{o3} the symmetry factors of the reduction reactions and the oxidation reaction, respectively, $E(t)$ in V the electrode potential and the time t in s.

With $\theta_S(t) + \theta_H(t) = 1$, the reaction rates $\nu(t)$ in mol cm^{-2} s^{-1} of each step of the overall reaction can be written by Equations (9) to (11):

$$\nu_1(t) = K_{r1}(t)\Gamma\left(1-\theta_H(t)\right) \tag{9}$$

$$\nu_2(t) = K_{r2}(t)\Gamma\left(\theta_H(t)\right) \tag{10}$$

$$\nu_3(t) = K_{o3}(t)\Gamma\left(1-\theta_H(t)\right) \tag{11}$$

with Γ in mol cm^{-2} the total number of adsorption sites per unit area, θ_H the covering factor of the adatom H, which is defined as H/Γ, where H in mol cm^{-2} is the surface concentration of the adatom H.

The Equation (12) of the evolution of the coverage rate $d\theta_H(t)/dt$ writes[1]:

$$d\theta_H(t)/dt = \nu_H(t)/\Gamma = -d\theta_s(t)/dt \tag{12}$$

with (Equation (13))

$$\nu_H(t) = \nu_1(t) - \nu_2(t) = -\nu_s(t) \tag{13}$$

Even though the rate of the oxidation reaction $\nu_3(t)$ does depend on the coverage rate of the adsorbed species, it does not affect its evolution as it consumes and produces an adsorption site. Hence, $\nu_H(t)$ and $\nu_s(t)$ depend solely on $\nu_1(t)$ and $\nu_2(t)$.

Finally, the Faradaic current $i_f(t)$ writes, Equation (14):

$$i_f(t) = -F\left(\nu_1(t) + \nu_2(t) - 2\nu_3(t)\right) \tag{14}$$

Steady-state kinetic equations

Steady-state equations are needed to determine the initial and final values of the potential, current and coverage rates.

[1] Please note the use of straight d for the derivatives as the coverage rates only depend on time.

Writing that at steady-state, Equation (15)

$$\mathrm{d}\theta_{\mathrm{H}}(t)/\mathrm{d}t = \mathrm{d}\theta_{\mathrm{s}}(t)/\mathrm{d}t = 0 \quad (15),$$

we have been using Equationss (9-15), to obtain Equations (16) and (17):

$$\theta_{\mathrm{H}}(E) = K_{\mathrm{r1}}(E)/\left(K_{\mathrm{r1}}(E)+K_{\mathrm{r2}}(E)\right) \quad (16)$$

$$i_{\mathrm{f}}(E) = \left(2F\Gamma\left(K_{\mathrm{o3}}(E)K_{\mathrm{r2}}(E)\text{-}K_{\mathrm{r1}}(E)K_{\mathrm{r2}}(E)\right)\right)/\left(K_{\mathrm{r1}}(E)+K_{\mathrm{r2}}(E)\right) \quad (17)$$

where E is the time-independent or steady-state potential.

The corrosion potential (Equation (18)), defined as the potential for a zero Faradaic current ($i_{\mathrm{f}}(E_{\mathrm{corr}}) = 0$), can be calculated from Equations (6) to (8) and (17):

$$E_{\mathrm{corr}} = \ln\left(k_{\mathrm{r1}}/k_{\mathrm{o3}}\right)/\left(\left(\alpha_{\mathrm{r1}}+2\alpha_{\mathrm{o3}}\right)f_{\mathrm{N}}\right) \quad (18)$$

Figure 1 below shows the steady-state Faradaic current and the coverage rate of the adatom H as a function of the steady-state potential E for a given set of kinetic parameters (shown in the caption of Fig. 1) and using Equations (6) to (8), (16) and (17). Two points are shown in Fig. 1, the initial steady-state potential E_{i} and the corrosion potential E_{corr} with their corresponding Faradaic current and coverage rates.

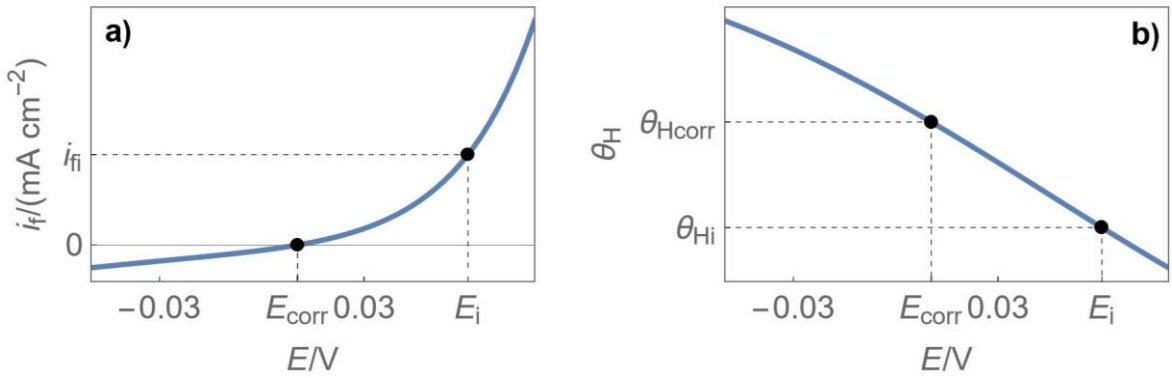

Figure 1. *Steady-state evolution of (a) the current and (b) the coverage rate of the adatom H as a function of the steady-state potential E. The parameters used to plot these curves are:* Γ*=10^{-9} mol cm^{-2},* f_N *= 38.9 V^{-1},* α_{r1} *= 0.7,* α_{r2} *= 0.3,* a_{o3} *= 0.5,* k_{r1} *= 2 s^{-1},* k_{r2} *=* k_{o3} *= 1 s^{-1},* E_i *=* E_{corr} *+ 0.05 V*

Steady-state Faradaic impedance

The steady-state Faradaic impedance of the Volmer-Heyrovský corrosion reaction Z_{f} is a sum of three terms [1,29], a charge transfer resistance and two surface concentration impedances related to adsorbed species s and H, Equation (19):

$$Z_{\mathrm{f}}(p) = R_{\mathrm{ct}} + Z_{\mathrm{s}}(p) + Z_{\mathrm{H}}(p) \quad (19)$$

with $p = 2\pi jf$, f in Hz the frequency and j the imaginary number such that $j^2 = -1$.

The details of the calculation will not be given here, but we have Equation (20):

$$Z_{\mathrm{f}}(p) = \frac{\left(K_{\mathrm{r2}}+K_{\mathrm{r1}}\right)\left(K_{\mathrm{r2}}+K_{\mathrm{r1}}+p\right)}{f_{\mathrm{N}}F\Gamma K_{\mathrm{r2}}\left(\alpha_{\mathrm{r1}}K_{\mathrm{r1}}\left(2\left(K_{\mathrm{o3}}+K_{\mathrm{r2}}\right)+p\right)+4\alpha_{\mathrm{o3}}K_{\mathrm{o3}}\left(K_{\mathrm{r2}}+K_{\mathrm{r1}}+p\right)+\alpha_{\mathrm{r2}}K_{\mathrm{r1}}\left(\text{-}2K_{\mathrm{o3}}+2K_{\mathrm{r1}}+p\right)\right)} \quad (20)$$

The structure of this impedance is equivalent to that of an $R + C/R$ circuit. To obtain the electrode impedance $Z(p)$ we need to add in parallel the double-layer capacitance C_{dl}. The ECM that can be used to model the impedance of the Volmer-Heyrovský corrosion reaction is shown in Fig. 2 with Equations (21) to (23):

$$R_{ct} = \frac{K_{r2} + K_{r1}}{f_N F \Gamma K_{r2}\left(4\alpha_{o3}K_{o3} + (\alpha_{r1} + \alpha_{r2})K_{r1}\right)} \tag{21}$$

$$R_\theta = \frac{K_{r1}\left(K_{r1} - K_{r2} - 2K_{o3}\right)R_{ct}\left(\alpha_{r1} - \alpha_{r2}\right)}{4\alpha_{o3}K_{o3}\left(K_{r2} + K_{r1}\right) + 2K_{o3}K_{r1}\left(\alpha_{r1} - \alpha_{r2}\right) + 2K_{r1}\left(\alpha_{r1}K_{r2} + \alpha_{r2}K_{r1}\right)} \tag{22}$$

$$C_\theta = \frac{4\alpha_{o3}K_{o3} + \alpha_{r1}K_{r1} + \alpha_{r2}K_{r2}}{K_{r1}\left(K_{r1} - K_{r2} - 2K_{o3}\right)R_{ct}\left(\alpha_{r1} - \alpha_{r2}\right)} \tag{23}$$

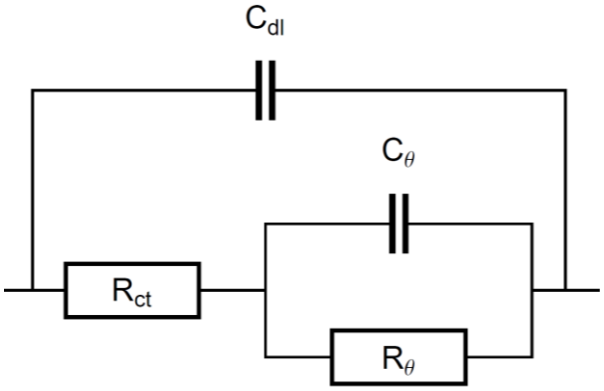

Figure 2. *ECM used to model the Volmer-Heyrovský corrosion reaction*

Finally, we have Equation (24):

$$Z(p) = Z_f(p) / (1 + Z_f(p) C_{dl} p) \tag{24}$$

with Equation (25)

$$Z_f(p) = R_{ct} + R_\theta / (1 + R_\theta C_\theta p) \tag{25}$$

Please note that the reaction rate constants K_{r1}, K_{r2} and K_{o3} are dependent on the potential according to Equations (6) to (8). Figure 3 shows two Nyquist diagrams of the impedance Z at two different potential values, E_i and the corrosion potential E_{corr}, using the same set of parameters as in Figure 1 and C_{dl} = 10 μF.

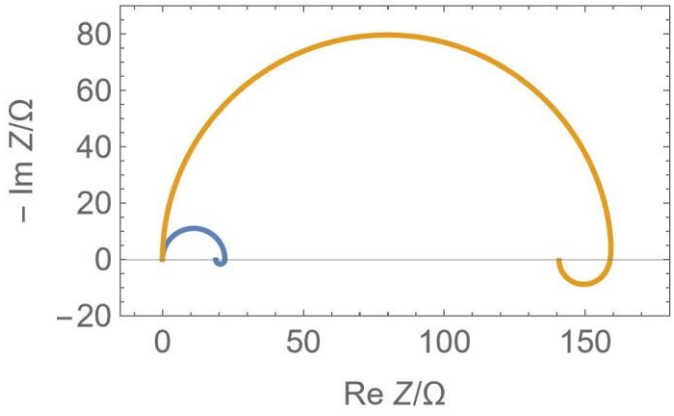

Figure 3. *Nyquist diagrams of the steady-state impedance Z at two different steady-state potentials E_i (blue curve) and E_{corr} (orange curve). The parameters used to plot these curves are: $\Gamma = 10^{-9}$ mol cm^{-2}, f_N = 38.9 V^{-1}, F = 96485 C mol^{-1}, α_{r1} = 0.7, α_{r2} = 0.3, a_{o3} = 0.5, $k_{r1} = 2\ s^{-1}$, $k_{r2} = k_{o3} = 1\ s^{-1}$, $E_i = E_{corr}$ + 0.05 V, C_{dl} = 10 μF, f_{min} =100 mHz, f_{max} = 10 kHz*

Simulated experiment and objectives of this work

As depicted in Fig. 4a, it consists of a simple current interrupt experiment: the electrochemical system, described by the Volmer-Heyrovský corrosion mechanism, is polarized at an anodic

potential E_i and a current i. At t = 0, the circuit is open and the potential decays to its other steady-state value, namely E_{corr}. The first objective of this work is to calculate the transient, non-stationary evolution of the potential between E_i and E_{corr}, as illustrated in Figure 4b.

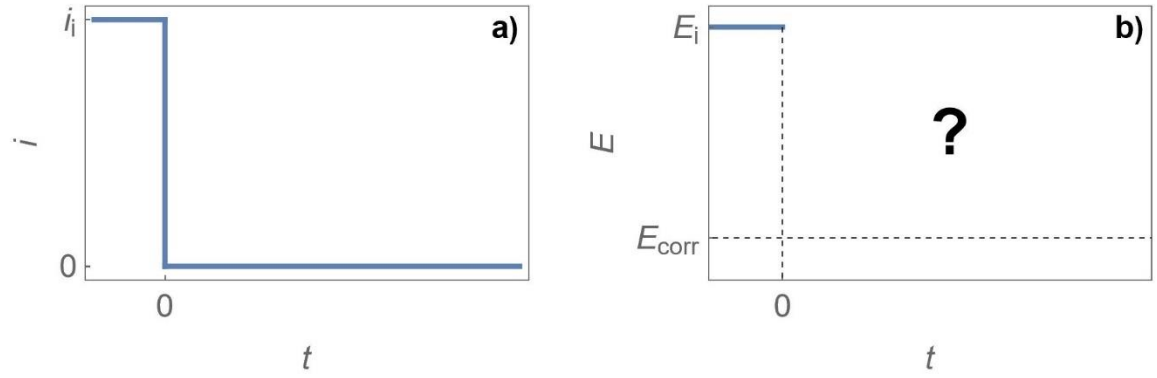

Figure 4. *Illustrative depiction of a) the current interrupt experiment and b) the unknown potential time evolution during its relaxation*

If the non-stationary time evolution of the potential $E(t)$ is known, it means the time evolution of the various reaction rate constants $K_{r1}(t)$, $K_{r2}(t)$ and $K_{o3}(t)$ can also be known.

A time- and frequency-dependent impedance $Z_f(p,t)$ can then be defined using the expression of the steady-state Faradaic impedance (Equation 20), which makes the reaction rate constant and time-dependent. Similarly, $R_{ct}(t)$, $R_\theta(t)$, $C_\theta(t)$ and $Z(p,t)$ can be defined and calculated by Equation (26).

$$Z(p,t) = Z_f(p,t) / (1 + Z_f(p,t) C_{dl} p) \tag{26}$$

The second objective of this work is to show the non-stationary impedance Nyquist diagrams during the relaxation of the system using Eq. (26).

$E(t)$ and $\theta_H(t)$ determination

Assuming zero Faradaic current

Our system of equations to solve is composed of an ordinary differential equation (ODE), which is Equation (12). Using Equations (9), (10) and (13) it writes Equation (27):

$$\mathrm{d}\theta_H(t) / \mathrm{d}t = K_{r1}(E(t))(1-\theta_H(t)) - K_{r2}(E(t))(\theta_H(t)) \tag{27}$$

During the relaxation experiment, it was first assumed that i_f = 0. We then used Equations (9) to (11) and (14) to obtain Equation (28).

$$K_{r1}(E(t))(1-\theta_H(t)) - K_{r2}(E(t))(\theta_H(t)) - 2K_{o3}(E(t))(1-\theta_H(t)) = 0 \tag{28}$$

Equations (27) and (28) constitute a differential algebraic system of equations (DAE), and which can be solved numerically.

The general form of a DAEs is presented by Equations (29) and (30):

$$\mathrm{d}x / \mathrm{d}t = f(x(t), y(t), t) \tag{29}$$

$$0 = g(x(t), y(t), t) \tag{30}$$

In our case, $x(t) = \theta_H(t)$ and $y(t) = E(t)$.

The NDSolve function in Mathematica 14 [30] was used to solve this DAE. The steady-state values were set as initial conditions $E(0) = E_i$ and $\theta_H(0) = \theta_H(E(0))$. The same parameters as in Figures 1 and

3 are used. In this case, the NDSolve function can only give a solution, an interpolation function defined for a given period (in our case 50 s), if the initial condition on the potential is not respected. This is shown in Figure 5: the initial potential is not E_{corr} + 0.05 V, which means the assumption needs to be revised. However, $\theta_H(t)$ seems to be correct.

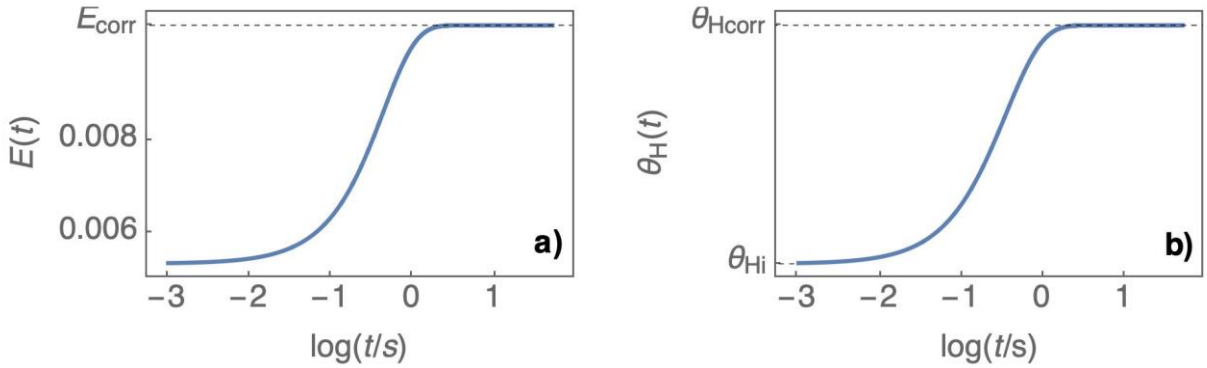

Figure 5. *Simulated (a)* E(t) *and (b)* θ_H(t) *assuming a zero Faradaic current during the relaxation. The solution for* E(t) *is wrong as it does not fulfill the initial condition* E*(0)* =E_i

Assuming zero total current

As the total current is the sum of the capacitive and the Faradaic current, assuming a zero total current during the relaxation leads to $i_c = -i_f$ and Equation (31):

$$C_{dl}\left(\frac{dE(t)}{dt}\right) = F\Gamma\left(K_{r1}\left(E(t)\right)\left(1-\theta_H(t)\right) - K_{r2}\left(E(t)\right)\left(\theta_H(t)\right) - 2K_{o3}\left(E(t)\right)\left(1-\theta_H(t)\right)\right) \quad (31)$$

which is an ODE and constitutes with Equation (27) an ODE system. Using again the NDSolve function in Mathematica, two interpolation functions are obtained that both fulfil the initial conditions (Fig. 6). It is noteworthy that the transient open circuit voltage (OCV) goes below the long-time limit E_{corr} and that $\theta_H(t)$ has the same shape as in Figure 5.

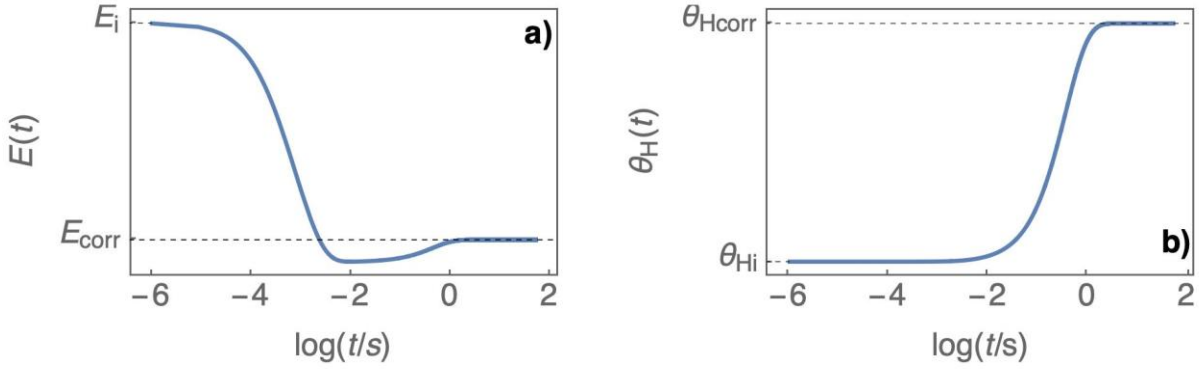

Figure 6. *Simulated (a) E(t) and (b)* $\theta_H(t)$ *assuming a total zero current during the relaxation. Both solutions fulfill the initial conditions* $\underline{E}(0) = E_i$ *and* $\theta_H(0) = \theta_H(E(0))$

Time-variant impedance

Now that $E(t)$ is known, $K_{r1}(t)$, $K_{r2}(t)$ and $K_{o3}(t)$, or more explicitly $K_{r1}(E(t))$, $K_{r2}(E(t))$ and $K_{o3}(E(t))$ can be caluclated. Introducing time in Equations (21) to (23) $R_{ct}(t)$, $R_\theta(t)$, the polarization resistance $R_p(t) = R_\theta(t) + R_{ct}(t)$ and $C_\theta(t)$ (Figure 7) can be computed.

One can note in Fig. 7 the negative signs of $R_\theta(t)$ and $C_\theta(t)$, which was to be expected considering the shape of the impedance diagram shown in Fig. 3, with a low-frequency inductive loop, typical of a Volmer-Heyrovský mechanism [1].

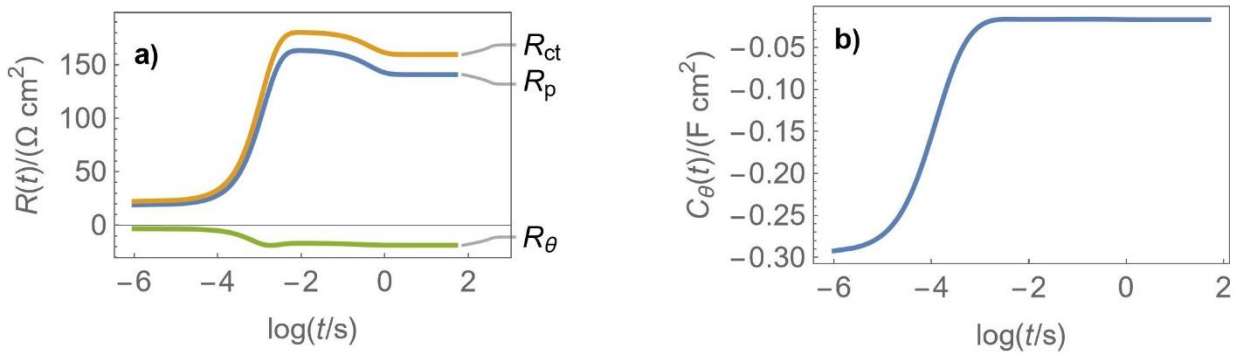

Figure 7. *Simulated (a)* $R_{ct}(t)$, $R_\theta(t)$ $R_p(t)$, *(b)* $C_\theta(t)$ *as a function of time during the relaxation of the OCV for the Volmer-Heyrovský corrosion mechanism using parameters shown in Figure 3*

To be able to plot the time-variant impedance measurement, for which, as a reminder, it is considered that the system is steady-state at each point, the time corresponding to each applied frequency needs to be calculated, considering that each frequency is applied sequentially from the highest to the lowest, which means we need to account for the accumulation of time.

Equation (32) was used:

$$t_k = \sum_{j=1}^{k} N(1+pw)T_j \tag{32}$$

with t_k the time corresponding to the k^{th} frequency, N the number of periods chosen for the measurement and pw a percentage of the period used as a waiting time to reduce inter-frequency transient regime, and T_j is the period of the j^{th} frequency.

A list of k frequencies f_k and the corresponding list of periods $T_k = 1/f_k$ were considered. Equation (32) above gives the list of the corresponding times t_k.

Table 1 gives values for 6 frequencies over a decade.

Table 1. *Numerical examples for the formula given in Equation (32) using* N *= 2 and* pw *= 10 %*

Rank *k*	*f*/Hz	*T*/s	*t*/s
1	100	0.01	0.022
2	68.13	0.015	0.054
3	46.42	0.022	0.102
4	31.62	0.032	0.171
5	21.54	0.046	0.273
6	14.68	0.068	0.423
7	10.00	0.10	0.643

Here we will try to discuss an inherent contradiction of our approach: the assumption that the system is stationary at each measurement allows us to use a Faradaic impedance expression derived from this assumption shown in Equation (20), in which a time-dependent term is "injected", here $E(t)$. In our previous paper [2], this assumption could be verified by low values of non-stationary distortion (NSD) indicators. However, if our system is stationary at each measurement point, how can it be non-stationary over the whole measurement?

The way we exit this contradiction is by saying that the negligibility of the time-variance at each point does not hold if all points are considered. In other terms, the small error conceded at each point accumulates over the whole spectrum and becomes non-negligible. This, of course, favors the use of input modulation made of simultaneous frequencies, as mentioned in the introduction. This is exactly what is referred to by quasi-stationarity: the system has a certain "level" of non-

stationarity that can, within certain conditions, be considered negligible. The same approach is used to consider linearity: an electrochemical system is nonlinear, but it is assumed that below a certain level, its non-linearity can be considered negligible.

In case the system is "strongly" non-stationary due to a fast scan rate, for example, in a DEIS experiment or a large charge/discharge current for a battery, our approach is not valid.

Similarly, if the system behaviour is strongly nonlinear due to a very large amplitude, the measured impedance cannot be analysed in terms of "classical" Faradaic impedance or with "classical" ECMs.

Figure 8 shows the Nyquist diagram of the time-variant electrode impedance corresponding to Equations 26 and 25 (Z_{TV}, black dots) and the two steady-state impedance graphs already shown in Figure 3 ($Z_{St,\,t=0}$, $Z_{St,\,t=tmax}$), which correspond to the impedance of the system in its initial and final state. The graph distortion is visible at mid-frequencies and corresponds to the change of parameters shown in Fig. 7.

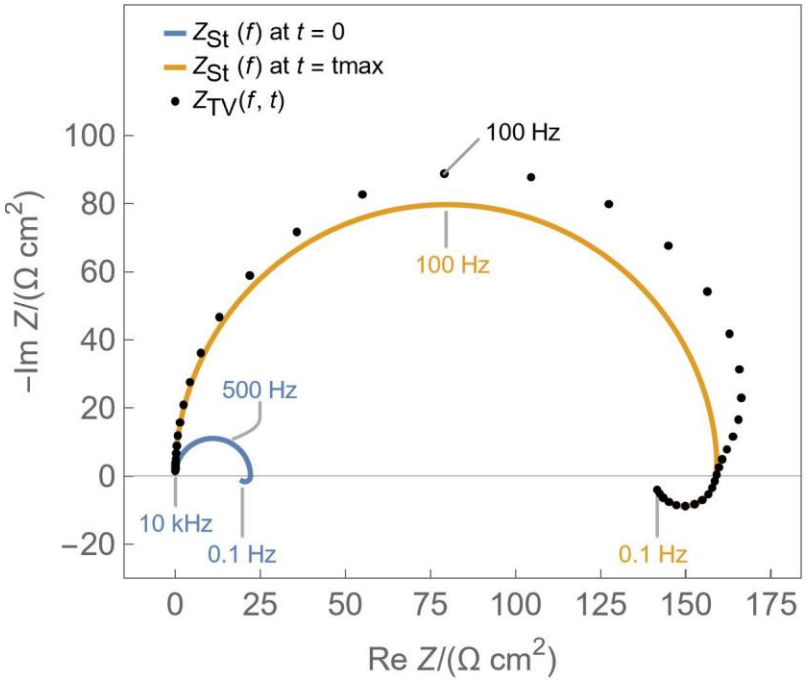

Figure 8. *Simulated Nyquist diagram of the time-variant impedance expression shown in Equation (26) in black dots. The orange and blue curves correspond to the two steady-state impedance graphs already shown in Figure 3, which correspond to the initial and final state of the system. The parameters are the same as in Figure 3, with 6 points per decade,* N *= 2 and* pw *= 10 %.*

The larger semi-circle at mid-frequencies corresponds to C_{dl}/R_{ct} and the low-frequency inductive loop to C_θ/R_θ. The kinetic constants and potential ranges were chosen to show a low-frequency inductive loop. For the Volmer-Heyrovský mechanism, low-frequency capacitive behaviour is expected at cathodic potentials [1,29]. The timescales shown in Figures 5 to 7 depend on the kinetic parameters chosen.

The second part of the paper will deal with the experimental validation of this theoretical approach.

Conclusion

Basically, in the literature, two approaches were adopted to deal with non-stationary impedance measurements: either a mathematical treatment and correction of the data or an adjustment of the input modulation such that the system is considered in a quasi-stationary state across the whole frequency range.

In this part of the paper, an approach based on the electrochemical reaction that takes place in the system under study was presented, for which the non-stationarity of the system can be calculated and accounted for in the Faradaic impedance expression.

The transient potential and coverage rate evolution during the relaxation of a system where the Volmer-Heyrovský corrosion mechanism takes place were calculated by solving a system of two ODEs written using the kinetic equations governing the reaction and assuming, during the relaxation, that the sum of the capacitive and Faradaic currents is equal to zero.

Stationary impedance expressions for this mechanism were given and converted into time and frequency-dependent expressions using the potential evolution previously determined. It was then possible to simulate the time and frequency-dependent impedance that would be measured during the relaxation. This approach removes the need to estimate or correct non-stationarity of the system, as it is "embedded" in the Faradaic impedance expression.

References

[1] J.-P. Diard, B. Le Gorrec, C. Montella, *Cinétique électrochimique*, Hermann, Paris, France, 1996 (in French). ISBN-13 : 978-2705662950

[2] N. Murer, J.-P. Diard, B. Petrescu, Time-variance in EIS measurements: the simple case of dilution, *Journal of The Electrochemical Society* **170** (2023) 126506-126517. https://doi.org/10.1149/1945-7111/ad1632

[3] N. Murer, J.-P. Diard, B. Petrescu, The effects of time-variance on impedance measurements: examples of a corroding electrode and a battery cell, *Journal of Electrochemical Science and Engineering* **10** (2020) 127-140. https:/

[4] /doi.org/10.5599/jese.725

[5] F. Seland, R. Tunold, D. A. Harrington, Impedance study of methanol oxidation on platinum electrodes, *Electrochimica Acta* **51** (2006) 3827-3840 https://doi.org/10.1016/j.electacta.2005.10.050

[6] M. Keddam, Z. Stoynov, H. Takenouti, Impedance measurement on Pb/H_2SO_4 batteries, *Journal of Applied Electrochemistry* **7** (1977) 539-544 https://doi.org/10.1007/BF00616766

[7] G. A. Ragoisha, A. S. Bondarenko, *Chemical problems of the development of new materials and technologies, Potentiodynamic electrochemical impedance spectroscopy*, Minsk, Belarus, 2003, 138-150 https://elib.bsu.by/bitstream/123456789/21022/1/pages%20from%20Sbornik-END9.pdf

[8] A. M. Bond, N. W. Duffy, D. M. Elton, B. D. Fleming, Characterization of nonlinear background components in voltammetry by use of large amplitude periodic perturbations and Fourier transform analysis, *Analytical Chemistry* **81** (2009) 8801-8808 https://doi.org/10.1021/ac901318r

[9] J. Schiewe, J. Házi, V. A. Vicente-Beckett, A. M. Bond, A unified approach to trace analysis and evaluation of electrode kinetics with fast Fourier transform electrochemical instrumentation, *Journal of Electroanalytical Chemistry* **451** (1998) 129-138 https://doi.org/10.1016/S0022-0728(97)00579-2

[10] M. J. Walters, J. E. Garland, C. M. Pettit, D. S. Zimmerman, D.R. Marr, D. Roy, Weak adsorption of anions on gold: measurement of partial charge transfer using Fast Fourier Transform electrochemical impedance spectroscopy, *Journal of Electroanalytical Chemistry* **499** (2001) 48-60 https://doi.org/10.1016/S0022-0728(00)00468-X

[11] T. Pajkossy, M. Urs Ceblin, G. Mészáros, Dynamic electrochemical impedance spectroscopy for the charge transfer rate measurement of the ferro/ferricyanide redox couple on gold, *Journal of Electroanalytical Chemistry* **899** (2021) 115655-115663 https://doi.org/10.1016/j.jelechem.2021.115655

[12] K. Darowicki, J. Orlikowski, G. Lentka, Instantaneous impedance spectra of a non-stationary model electrical system, *Journal of Electroanalytical Chemistry* **486** (2000) 106-110 https://doi.org/10.1016/S0022-0728(00)00111-X

[13] Z. Stoynov, B. Savova, Instrumental error in impedance measurements of non-steady-state systems, *Journal of Electroanalytical Chemistry* **112** (1980) 157-161 https://doi.org/10.1016/S0022-0728(80)80016-7

[14] Z. B. Stoynov, B. S. Savova-Stoynov, Impedance study of non-stationary systems: four-dimensional analysis, *Journal of Electroanalytical Chemistry* **183** (1985) 133-144 https://doi.org/10.1016/0368-1874(85)85486-1

[15] Z. Stoynov, B. Savova-Stoynov, Non-stationary impedance analysis of lead/acid batteries, *Journal of Power Sources* **30** (1990) 275-285 https://doi.org/10.1016/0378-7753(93)80085-4

[16] Z. B. Stoynov, Rotating Fourier transform: new mathematical basis for non-stationary impedance analysis, *Electrochimica Acta* **37** (1992) 2357-2359 https://doi.org/10.1016/0013-4686(92)85132-5

[17] Z. B. Stoynov, Non-stationary impedance spectroscopy, *Electrochimica Acta* **38** (1993) 1919-1922 https://doi.org/10.1016/0013-4686(93)80315-Q

[18] E. Van Gheem, R. Pintelon, J. Vereecken, J. Schoukens, A. Hubin, P. Verboven, O. Blajiev, Electrochemical impedance spectroscopy in the presence of nonlinear distortions and non-stationary behaviour Part I: theory and validation, *Electrochimica Acta* **49** (2004) 4753-4762 https://doi.org/10.1016/j.electacta.2004.05.039

[19] E. Van Gheem, R. Pintelon, A. Hubin, J. Schoukens, P. Verboven, O. Blajiev, J. Vereecken, Electrochemical impedance spectroscopy in the presence of nonlinear distortions and non-stationary behaviour Part II. Application to crystallographic pitting corrosion of aluminium, *Electrochimica Acta* **51** (2006) 1443-1452 https://doi.org/10.1016/j.electacta.2005.02.096

[20] Systems and EIS quality indicators, https://www.biologic.net/wp-content/uploads/2019/08/systems-and-eis-quality-indicators-wp2-electrochemistry.pdf (26/7/2024)

[21] N. Hallemans, D. Howey, A. Battistel, N. F. Saniee, F. Scarpioni, B. Wouters, F. La Mantia, A. Hubin, W. D. Widanage, J. Lataire, Electrochemical impedance spectroscopy beyond linearity and stationarity, *Electrochimica Acta* **466** (2023) 142939-142962. https://doi.org/10.1016/j.electacta.2023.142939

[22] K. J. Szekeres, S. Vesztergom, M. Ujvári, G. G. Láng, Methods for the determination of valid impedance spectra in non-stationary electrochemical systems: concepts and techniques of practical importance, *ChemElectroChem* **8** (2021) 1233-1250 https://doi.org/10.1002/celc.202100093

[23] R. Pachimatla, M. Thomas, S. Rahman OC, R. Srinivasan, Analysis of instabilities in electrochemical systems using nonlinear electrochemical impedance spectroscopy, *Journal of The Electrochemical Society* **166** (2019) H304-H312 https://doi.org/10.1149/2.0571908jes

[24] F. Berthier, *Spectroscopie d'impédance et vitesse de corrosion : application au cas de la corrosion du zinc en milieu NaCl 3 %*, Ph. D. Thesis, INP Grenoble (1989) (in French)

[25] M. Baddi, *Vérification d'un modèle réactionnel de passivation du fer en milieu acide*, Ph. D. Thesis, Université Pierre et Marie Curie Paris VI (1977) (in French)

[26] D. A. Harrington, B. E. Conway, Kinetic theory of the open-circuit potential decay method for evaluation of adsorbed intermediates: Analysis for the case of the H_2 evolution reaction, *Journal of Electroanalytical Chemistry* **221** (1987) 1-21 https://doi.org/10.1016/0022-0728(87)80242-5

[27] J. Heyrovský, A theory of overpotential, *Recueil des travaux chimiques des Pays-Bas* **46** (1927) 582-586 https://doi.org/10.1002/recl.19270460805

[28] T. Erdey-Grúz, M. Volmer, Zur Theorie der Wasserstoff Überspannung, *Zeitschrift für Physikalische Chemie* **150A** (1930) 203-213 (in German) https://doi.org/10.1515/zpch-1930-15020

[29] J. Huang, Correlation between electrocatalytic activity and impedance shape: A Theoretical Analysis, *PRX Energy* **3** (2024) 023001. http://doi.org/10.1103/PRXEnergy.3.023001

[30] J.-P. Diard, C. Montella, N. Murer. *Handbook of electrochemical impedance spectroscopy corrosion reactions library,* Self-published, Seyssinet-Pariset, France, 2012, p. 11 https://doi.org/10.13140/RG.2.2.16871.87206

[31] Wolfram Language & System Documentation Center https://reference.wolfram.com/language/ref/NDSolve.html (31/7/2024)